GEOLOGICKÝ ZBORNÍK — GEOLOGICA CARPATHICA, 35, 3, BRATISLAVA, JUNE 1984
Pp. 329—354

LEONID LVOVICH PERCHUK*

THEORETICAL CONSIDERATION OF BASALT SERIES: TEMPERATURE CONTROL

(Figs. 12, Tabs. 6)

A b s t r a c t: Numerous experimental data for dry systems of various compositions with olivine-forsterite or fayalite on cotectic were thermodynamically treated using the V a n L a a r law. The linear relationship between $\ln X^*_{ol}$ and 1/T which was found in the Na_2O and K_2O-free system made it possible to calculate the melting enthalpies for these minerals and to establish temperature dependence for a mole fraction of potential olivine of a given composition in a rock

$$t\,°C = 10^6/675.536 - 23.6382\ X^{ol}_{Mg} - 114.5707641 \log X^{*}_{ol} - $$
$$- 0.018646(100\ X^{ol}_{Mg})^2 - 0.2796 \log X^{*}_{ol}\ (100\ X^{ol}_{Mg})^2 +$$
$$+ 0.000045 \log X^{*}_{ol}\ (100\ ^{ol}_{Mg})^3 - 333 - 220 \log X^{*}_{ol},$$

where X^{ol}_{Mg} is the forsterite mole fraction in olivine; X^{*}_{ol} is the mole fraction of potential olivine in a rock. Still another equation gives the liquidus temperature

$$t\,°C = 1039.62 + 43.7368\ X^{ol}_{Mg} + 353.86\ y + 0.001182(100\ X^{ol}_{Mg})^2 +$$
$$+ 0.125186\ y(100\ X^{ol}_{Mg})^2 - 0.000031\ y(100\ X^{*}_{ol})^3,$$

where $y = (Mg + Fe + Mn)/1/2\ O_2$. The expression $X^{ol}_{Mg} = 3.15\ X^{rock}_{Mg})$ $(1 + 2.15\ X^{rock}_{Mg})$ from R o e d e r's experimental data helped to evaluate approximately the rock liquidus temperatures straight from bulk chemical analyses.

Chemical compositions of basic and ultrabasic rocks were calculated in hundreds with use of these equations, and cotectic minima were outlined in the alkali-silica diagrams for the magma series distinguished by K u n o (1960, 1968). The shift in the basalt cotectic minimum under the pressure and alkalinity of juvenile fluids can be seen, for example, in several continental volcanic formations. The intersection of liquidus projections at one point on the alkali-silica plot suggests a common source for the basalt series — the ultrabasic mantle of lherzolite with 42 — 44 wt.% of SiO_2 and $Na_2O + K_2O \approx 1{,}2$ wt.%. Alpino-type hyperbasites and many meimechites, kimberlites and peridotites contain less alkali, which suggests their restite origin.

* Prof. Dr. L. L. P e r c h u k, Institute of Experimental Mineralogy of the Acad. Sci., USSR, 142 432 Chernogolovka, Moscow Region.

The bi-pyroxene equilibrium has been studied on the FeO fractionation between phases which depends on their overall Mg/(Mg + Fe) ratio. An equation has been worked out, relating the constant of the FeO fractionation between Cpx and Opx, $\bar{X}_{Mg} = 1/2(X^{Opx} + X^{Cpx}_{Mg})$ and temperature. It gives us the subsolidus equilibrium temperatures in nodules from basalts and kimberlites as well as in certain magmatic rocks.

Р е з ю м е: Многочисленные экспериментальные данные для сухих систем разных составов с оливином — форстеритом или фаялитом на котектике были термодинамически обработаны при помощи закона Ван Лара. Линейное отношение между $\ln X^{*}_{01}$ и $1/T$ обнаруженное в свободном системе $Na_2O - K_2O$ предоставило возможность вычислению энтальпий плавления для этих минералов и установлению зависимости температуры для мольной доли потенциального оливина данного состава в породе

$$t\,^{\circ}C = 10^{4}/675{,}536 - 23{,}6382\ X^{01}_{Mg} - 114{,}5707641\ \log X^{*}_{01} - \\ - 0{,}018646\ (100\ X^{01}_{Mg})^2 - 0{,}2796\ \log X^{*}_{01}\ (100\ X^{01}_{Mg})^2 + \\ + 0{,}000045\ \log X^{*}_{01}\ (100^{01}_{Mg})^3 - 333 - 220\ \log X^{*}_{01},$$

где X^{01}_{Mg} — форстеритовая мольная доля в оливине; X^{*}_{01} — мольная доля потенциального оливина в породе. Другое уравнение дает температуру ликвидуса

$$t\,^{\circ}C = 1039{,}62 + 43{,}7368\ X^{01}_{Mg} + 353{,}86\ y + 0{,}001182\ (100\ X^{01}_{Mg})^2 + \\ + 0{,}125186\ y\ (100\ X^{01}_{Mg})^2 - 0{,}000031\ y\ (100\ X^{*}_{01})^3,$$

где $y = (Mg + Fe + Mn)/1\,2\,O_2$. Выражение $X^{01}_{Mg} = 3{,}15\ X^{пор.}_{Mg}\ (1 + 2{,}15\ X^{пор.}_{Mg})$ из экспериментальных данных Родера помогло приблизительно определить температуры жидкостей пород прямо из валовых химических анализов.

Химические составы основных и ультраосновных пород были вычислены в сотнях при помощи уравнений и котектические минимумы были набросанны в диаграммах щелочи-кремнезем для магматических серий выделеных Куно (1960,1968). Наблюдается сдвиг базальтового котектического минимума под влиянием давления и щелочности ювенильных жидкостей, например в нескольких континентальных вулканических формациях. Пересечение проекций ликвидусов в одном пункте на графике щелочи — кремнезем намекает общий источник базальтовых серий — ультраосновную мантию лерцолита с 42—44 весовыми процентами SiO_2 и $Na_2O + K_2O \approx 1{,}2$ вес. процентов. Альпиотипные гипербазиты и много меймечитов, кимберлитов и перидотитов содержат меньше щелочей, что говорит об их реститовом происхождении.

Двухпироксеновое равновесие было изучено на FeO фракционации между фазами, зависящей от их общего Mg/(Mg + Fe) отношения. Было составлено уравнение, которое определяет отношение константы FeO фракционации между Cpx и Opx, $\bar{X}_{Mg} = 1/2\ (X^{Opx} + X^{Cpx}_{Mg})$ и температурой. Оно дает нам температуры субсолидного равновесия в нодулях из базальтов и кимберлитов, а также в определенных магматических породах.

Introduction

The crystallization and differentiation of basic magmas have always been of crucial importance in petrology. Field and experimental evidence accumulated over the last 25 years enabled petrologists to detect a number of very important effects that elucidate the patterns of the formation of magmatic series of basic and ultrabasic rocks (Yoder and Tilley, 1962; Green and Ringwood, 1967, 1970; Engel et al., 1965; Zimin, 1973; Kutolin, 1972; Scheinmann, 1968; Hess, ed. 1968; Wyllie, ed. 1967). Kuno (1960) has also shown that the alkali and tholeiite basalt series have relatively constant $SiO_2/(Na_2O + K_2O)$. In a diagram bounded by these coordinates the boundary between these series is given by the constant ratio $SiO_2(Na_2O + K_2O) \approx 12 - 13$, to which high-alumina basalts correspond. This value is somewhat lower, ≈ 5—10, for the alkali rock series.

An analysis of the differentiation patterns will benefit greatly if the temperature regime of magmatic rock series formation at one particular depth is known (P≈const). Its importance is self-evident, because a decreasing temperature is the principal factor in differentiation by crystallization. It is therefore the purpose of our study to find the crystallization temperatures for each of the magmatic rocks.

There are several ways for calculating the crystallization temperatures and pressures of basic and ultrabasic rocks (Ramberg — De-Vore, 1951; Davis — Boyd, 1966; Kretz, 1963; Boyd, 1969; Roeder, 1974; Roeder — Emsley, 1970; Perchuk, 1968, 1970, 1973; MacGregor, 1974; Munoz — Sagredo, 1974, and others).

We have made an attempt to derive certain equations and diagrams for evaluating liquidus and subsolidus temperatures of basic and ultrabasic rocks. The obtained estimates are used for establishing certain overall patterns in the differentiation and crystallization of basic magmas.

The relation between the melt and the composition of the equilibrium phase crystallizing therefrom is described by the Van-Laar equation.

$$\ln a_i^{Liq} = \ln a_i^{Min} + \frac{\Delta H_i}{R}\left(\frac{1}{T_o} - \frac{1}{T}\right) \tag{1}$$

$$a_i = X_{i\gamma i} \tag{2}$$

Symbols

X_i^* — mole fraction of component i in the real cotectic melt,
X_i^o — mole fraction of component i in the ideal cotectic melt;
γ_i^* — accepted activity coefficient, equal to X_i/X_i^o;
a_i^{Liq} — activity of component i in the melt;
T — temperature, °K;
T_O — the melting temperature of the given pure substance;
ΔH_i^o — the melting heat of the pure substance;

G_i^{e*} — excess partial molar free Gibbs energy (provisional value, connected with γ_i^*);
t — temperature, °C;

$X^* NaAlSi_{1+n}O_{4+2n}$ — mole fraction of Ab or Ne in the melt = $Na_2O/SiO_2 + TiO_2 + Fe_2O_3 - Al_2O_3 - 4(Na_2O + K_2O)$.

Ab	— albite	Hem	— hematite
Am	— amphibole	Il	— ilmenite
An	— anorthite	Liq	— liquid
Bi	— biotite	Min	— mineral
Cd	— corundum	Mt	— magnetite
Cor	— cordierite	Ne	— nepheline
Ca-Cpx	— clinopyroxene	Ol	— olivine
Di	— diopside	Opx	— orthopyroxene
En	— enstatite	Pyr	— pyrope
Fo	— forsterite	Qz	— quartz
Fs	— ferrosilite	Ru	— rutile
Fsp	— alkali feldspar	Sp	— spinel
Gr	— garnet	Wu	— wustite

If the mineral separating from the solution is constant in composition, eq. (1) reduces to:

$$\ln a_i^{Liq} = \frac{\Delta H_i}{R}\left(\frac{1}{T_0} - \frac{1}{T}\right) \tag{3}$$

At ΔH_i = const, the $\ln a_i^{Liq}$ — 1/T is linear; the melt approaches an ideal solution, i. e. $\gamma_i = 1$ and

$$\ln X_i^{Liq} = \frac{\Delta H_i^0}{R}\left(\frac{1}{T_0} - \frac{1}{T}\right) \tag{4}$$

This expression can be used for thermodynamic calculating the experimental diagrams for complex systems without isomorphous solid mixtures. If the relationship $\ln a_i$ — 1/T is universal, it can be used in estimating the melting points of the pure components:

$$\Delta H_i^0 = \frac{TT_0R \ln X_i^{Liq}}{T - T_0} \tag{5}$$

which makes it possible to move ahead to the calculation of the diagrams — mineralogical thermometers. Here it becomes necessary to derive a general expression for X_i^{Liq} which would not depend on the molecular composition of

Table 1

Temperature of the beginning of forsterite crystallization in simple systems as determined from experimental data (Minerals, 1974)

No.	System	Composition	t °C	$\frac{10^3}{t+273}$	X^{Liq}_{Fo}	$-\log X^{*}_{Fo}$	$\left[\frac{\gamma^{*}_{Fo}}{10^{1-}}\right]$	X^{*}_{Na}	$X_{Ne(Ab)}$	Y
1	Fo-Cor	$Fo_{36}Cor_{64}$	1420	0.591	0.512	0.290	1.0	—	—	0.244
2		$Fo_{50}Cor_{50}$	1400	0.598	0.467	0.330	1.0	—	—	0.298
3	Fo-An-Qz	$Fo_{28}An_{50}Qz_{22}$	1260	0.652	0.290	0.538	1.0	—	—	0.133
4		$Fo_{33}An_{57}Qz_{10}$	1320	0.628	0.341	0.467	1.0	—	—	0.161
5	Fo-Di	$Fo_{40}Di_{60}$	1600	0.534	0.621	0.207	1.0	—	—	0.302
6		$Fo_{30}Di_{70}$	1550	0.549	0.554	0.256	1.0	—	—	0.268
7		$Fo_{20}Di_{80}$	1450	0.580	0.489	0.311	1.0	—	—	0.234
8		$Fo_{14}Di_{86}$	1400	0.598	0.448	0.349	1.0	—	—	0.214
9	$MgO-Al_2O_3-SiO_2$	56:16, 5:27,5	1700	0.507	0.647	0.189	1.0	—	—	0.498
10	$MgO-Al_2O_3-SiO_2$	25:24:51	1370	0.609	0.437	0.359	1.0	—	—	0.205
11	Fo-Qz	Fo_{100}	1890	0.462	1.000	0	1.0	—	—	0.500
12		$Fo_{90}Qz_{10}$	1850	0.471	0.899	0.046	1.0	—	—	0.442
13		$Fo_{80}Qz_{20}$	1735	0.498	0.800	0.097	1.0	—	—	0.386
14		$Fo_{70}Qz_{30}$	1610	0.531	0.698	0.156	1.0	—	—	0.332
15	Fo-Ab-Di	$Fo_{2.5}Ab_{97.5}$	1100	0.728	0.025	1.600	6.369	0.075	0.975	0.011
16		$Fo_{14}Ab_{18.5}Di_{67.5}$	1355	0.614	0.378	0.422	0.99	0.015	0.195	0.180
17		$Fo_{10}Ab_{50}Di_{40}$	1300	0.636	0.237	0.625	1.364	0.040	0.514	0.112
18		$Fo_8Ab_{69}Di_{23}$	1265	0.650	0.157	0.804	2.119	0.054	0.702	0.073
19		$Fo_5Ab_{86}Di_9$	1195	0.681	0.086	1.066	3.571	0.066	0.858	0.036
20	Di-Fo-Pyr	$Di_{46.5}Fo_5Pyr_{48.5}$	1490	0.567	0.471	0.327	1.0	—	—	0.224
21		$Di_{44}Fo_{10}Pyr_{46}$	1495	0.566	0.500	0.301	1.0	—	—	0.239
22		$Di_{41}Fo_{15}Pyr_{44}$	1515	0.559	0.530	0.276	1.0	—	—	0.254
23		$Di_{36}Fo_{10}Pyr_{54}$	1500	0.564	0.514	0.289	1.0	—	—	0.245
24	Di-Fo	$Di_{88}Fo_{12}$	1388	0.602	0.442	0.355	1.0	—	—	0.207
25		$Di_{78}Fo_{22}$	1480	0.570	0.501	0.300	1.0	—	—	0.241
26		$Di_{80}Fo_{20}$	1470	0.574	0.487	0.312	1.0	—	—	0.198
27	Di-Fo-Qz	$Di_{60}Fo_{25}Qz_{15}$	1411	0.594	0.481	0.318	1.0	—	—	0.220
28		$Di_{78}Fo_{12}Qz_{10}$	1390	0.601	0.450	0.347	1.0	—	—	0.089
29	Di-Pyr	$Di_{50}Pyr_{50}$	1450	0.580	0.449	0.348	1.0	—	—	0.229
30		$Di_{80}Pyr_{20}$	1375	0.607	0.393	0.405	1.0	—	—	0.202
31	Ne-Di	$Ne_{62}Di_{38}$	1200	0.679	0.128	0.892	1.805	0.091	0.637	0.062
32		$Ne_{32}Di_{68}$	1250	0.657	0.233	0.633	1.216	0.048	0.336	0.112
33		$Ne_{20}Di_{80}$	1295	0.638	0.276	0.559	1.161	0.030	0.210	0.133
34		$Ne_{60}Di_{40}$	1185	0.686	0.135	0.871	1.712	0.088	0.616	0.065
35	Ne-Di-Qz	$Ne_{59}Di_{28}Qz_{12}$	1140	0.708	0.094	1.027	2.169	0.085	0.595	0.045
36	Fo-Cor-Ab	$Fo_{19}Cor_{70}Ab_{5.5}$	1300	0.636	0.193	0.714	1.681	0.045	0.585	0.134

the system. This expression could be presented as an atomic fraction of compound (component) i relative to the total number of atoms in the system S:

$(\Sigma A_s = \Sigma A_i + \Sigma A_j)$:

$$X_i^{Liq} = \sum_i A_i / (\sum_j A_j + \sum_i A_i),$$

that is

$$X_i^{Liq} = \sum_i A_i / \sum_s A_s. \quad (6)$$

Even if the melt is not an ideal solution, the thermodynamic treatment of the experimental data will enable us to find both the activity coefficients and variations in the ΔH_i with the temperature and the composition of the melt.

The system olivine - melt

Consider iron-free melting systems. Tab. 1 summarizes the compositions of various systems and the temperatures of forsterite appearance on the liquidus, as well as certain compositional parameters of these systems. Tab. 2 presents the values for the forsterite fraction in the composite melt.

Table 2

Calculation of the olivine fraction in the melt $Ne_{59}Di_{28}Qz_{13}$

Compound	Wt. %	Mol./wt	Mol. quant. × 100	Mg	Si	O	Na	Al	Ca	Σ
$NaAlSiO_4$	59	142.02	415	0	415	1660	415	415	0	2905
$CaMgSi_2O_6$	28	216.52	129	129	258	774	0	0	129	1290
SiO_2	13	60.06	216	0	216	432	0	0	0	648
Mg_2SiO_4				129	64.5	258				4843

$$X^{Liq}_{Mg_2SiO_4} = 3.5Mg : \sum_s A_s = 451:4843 = 0.093$$

The diagram in Fig. 1 plots the-log X^{Liq}_{For} against the temperature (10^3/T) from the data in Tab. 1*. A distinct linear relation only appears between these parameters for Na-free systems, which implies that these melts approach ideal solutions. Addition of alkalis results in deviations from ideality, which

* Tab. 2 gives an example of such a calculation.

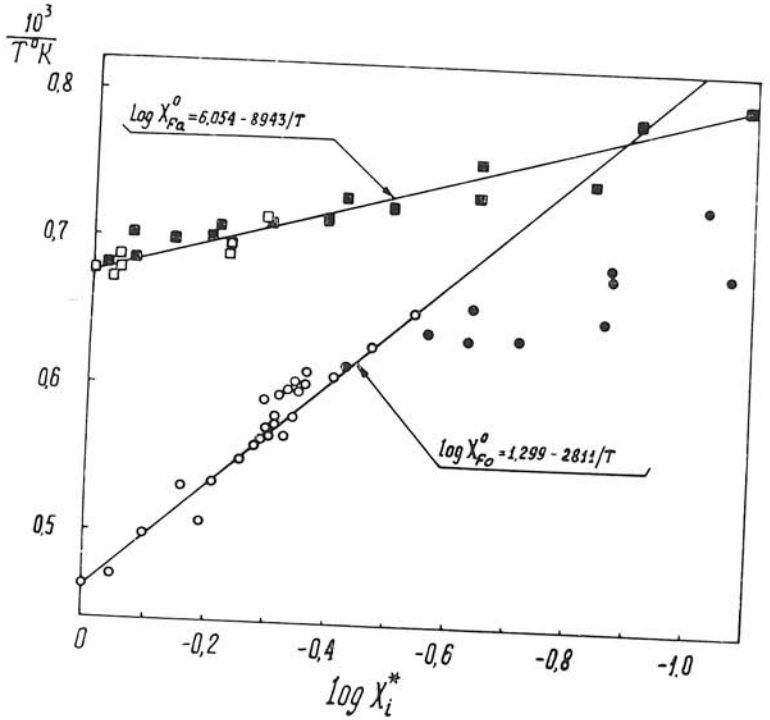

Fig. 1. The logarithm of mole fractions of forsterite and fayalite in cotectic melts vs. reciprocal temperature. Open signs are the alkali-free systems; black signs are the alkali-containing systems.

can be assessed quantitatively. Towards this end we calculate $\Delta H^{O}_{Mg_2SiO_4}$ in alkali-free melts. The Fo melting heat has been obtained by eq. (5) from the $\log_{10} X^{O}_{Fo}$ — 1/T linear relationship (Fig. 1)

$$\Delta H^{O}_{Mg_2SiO_4} = 14232 \text{ cal/mole} \tag{7}$$

The relation between $X^{O}_{Mg_2SiO_4}$ and inverse temperature is given by:

$$\log_{10} X^{O}_{Mg_2SiO_4} = 1.299 - 2811/T \tag{8}$$

In the diagram of Fig. 1 the points for the Na_2O-containing systems lie to the right of the line given by this equation. It means that at X^{O}_{Fo} = const.

the temperatures of Fo crystallization from the alkaline melt are higher than the respective temperatures in any other alkali-free magma. The higher temperatures of the forsterite separation on the cotectic line of the alkali-bearing system are due to acid-base interaction of components in dry silicate melts (Korzhinskii, 1959; Kushiro, 1975). Thermodynamically this effect could be explained by the fact that these melts are far from being ideal solutions and, consequently, show higher-temperature heterogenezation. The activity coefficient γ_i of component i or its excess partial molar free Gibbs energy are known to be a measure of this deviation:

$$G_i^e = RT \ln \gamma_i, \tag{9}$$

With this value we shall be able to account for the acidbase interaction of the components (Korzhinskii, 1959; Kushiro, 1973) by introducing a correction for this effect in the calculated t °C. From the experimental data available, the direct estimates of the Mg_2SiO_4 activity coefficient present certain difficulties. So we introduced an equivalent value, the provisional Fo activity coefficient, in the melt

$$\overset{*}{\gamma}_{Mg_2SiO_4} = \left[\frac{X^{O}_{Mg_2SiO_4}}{X^{*}_{Mg_2SiO_4}}\right]^{Liq} = \exp\left[\frac{(G^{e}_{Fo})^{*}}{RT}\right]^{Liq}, \tag{10}$$

where $X^{*}_{Mg_2SiO_4}$ is the mole fraction of forsterite component in the alkali-bearing melt, $X^{O}_{Mg_2SiO_4}$ is the same in the alkalifree melt. The temperature dependence of this mole fraction is described by eq. (8). By turning this equation around and substituting it into (10), we obtain

$$\overset{*}{\gamma}_{Mg_2SiO_4} = [\exp_{10}(1.299 - 2811)/T]/X^{*}_{Mg_2SiO_4} \tag{11}$$

where

$$G^{e}_{Mg_2SiO_4} = RT \ln \overset{*}{\gamma}_{Mg_2SiO_4} \tag{12}$$

Column 8 of Tab. 1 gives the provisional activity coefficients of Fo in the alkali-bearing melts, which were calculated by eq. (11). They indicate the magnitude by which this system deviates from "ideal" melts at each given temperature. If these values actually have this physical meaning, they must be strongly dependent on the temperature and composition of the system.

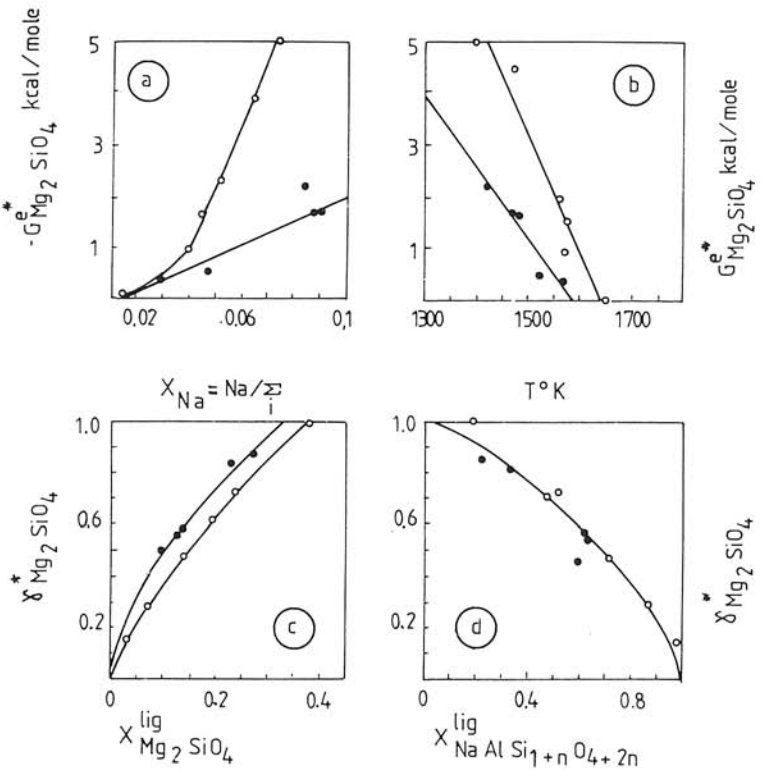

Fig. 2. The dependence of $G^{e*}_{Mg_2SiO_4}$ and $\gamma_{Mg_2SiO_4}$ on temperature and composition of cotectic melts. Open circles are for the systems with albite; black circles are for the systems with nepheline.

This relationship has been plotted in the diagrams (Fig. 2) from the data in Tab. 1. We were surprised to find greater deviations of cotectic melts from the "ideal" in albite-bearing than in nepheline-bearing systems. However, the diagram "d" in Fig. 2 shows the universal dependence of $\gamma^*_{Mg_2SiO_4}$ and

$(G^{e}_{Mg_2SiO_4})^*$ values on the $NaAlSi_3O_8$ or $NaAlSiO_4$ contents in cotectic association. This dependence is described by exponential series

$$\overset{*}{\gamma}_{Mg_2SiO_4} = (1.00051 - 0.1806\,X - 0.49561\,X^2 - 3.06639\,X^3 + 6.08234\,X^4 - 3.3072\,X^5), \quad (13)$$

where X is the Ab or Ne mole fraction in the system.

Now consider the data on fayalite melting in the simple Mg-free system. Tab. 3 gives the compositions of such systems and also the fayalite melting temperatures on the cotectic.

The diagram in Fig. 1 shows the linear relationship between $\log X^{O}_{Fe_2SiO_4}$ and inverse temperature. This dependence is described by equation

$$\log X^{O}_{Fe_2SiO_4} - 6.054 - 8943/T. \quad (14)$$

Consequently even alkaline melts approach "ideal" melts at the mean fayalite melting heat

$$\Delta H^{O}_{Fe_2SiO_4} = 29670 \text{ cal/mole} \quad (15)$$

At the overal linear relationship $\log X^{O}_{Fe_2SiO_4} - 10^3/T$, the system Fa—Ab begins to show a deviation from the ideal in both directions, as the provisional activity coefficients calculated for the system indicate. Tab. 3 and the diagrams in Fig. 3 show that the activity coefficients of Fe_2SiO_4 in the melt depend on the composition of this melt: the dependence reveals a slight deviation from the ideal solution in both directions. We failed to establish similar distinct dependences in the systems Ne-Wu-Qz-and Qz-Wu-Cd.

In the pure system $Fe_2SiO_4 - Mg_2SiO_4$ the melting proceeds according to Bowen and Schairer's diagram (1935). With this we can calibrate the diagram in Fig. 1, i. e. locate the positions of the lines for a constant composition of equilibrium phases. To do this we must expect the olivine melting heat to vary proportionally with the Mg/Mg + Fe ratio. If this is so, all the lines for equal compositions of olivine in equilibrium with the melt of a given composition will intersect at the same point at which the temperature dependence lines for $\log X^{O}_{Mg_2SiO_4}$ and $\log X^{O}_{Fe_2SiO_4}$ do.

Fig. 4 is a variant of the diagram drawn up on this assumption. The abscissa

Table 3

Initial crystallization temperature of tayalite in simple systems as determined from experimental data (Minerals, 1974)

No.	System	Composition (wt. %)	$\frac{10^3}{t+273}$	t° C	X^*_{Fa}	$-\log X^*_{Fo}$	$1/\gamma^*_{Fa}$	X^*_{Na}	$X^*_{Ab\ (Ne)}$	Fe $1/2\ O_2$
1		$Ab_{80}Fa_{20}$	0.774	1070	0.142	0.8316	1.770	0.0656	0.852	0.069
2		$Ab_{70}Fa_{30}$	0.733	1090	0.229	0.6409	1.377	0.0593	0.771	0.108
3		$Ab_{60}Fa_{40}$	0.723	1110	0.310	0.5010	1.225	0.0525	0.678	0.150
4		$Ab_{50}Fa_{50}$	0.717	1120	0.409	0.3884	1.072	0.0454	0.590	0.195
5	Ab-Fa	$Ab_{40}Fa_{60}$	0.712	1130	0.509	0.2932	0.954	0.0376	0.489	0.245
6		$Ab_{30}Fa_{70}$	0.707	1140	0.617	0.2095	0.873	0.0293	0.381	0.300
7		$Ab_{20}Fa_{80}$	0.695	1165	0.734	0.1314	0.940	0.0203	0.264	0.360
8		$Ab_{10}Fa_{90}$	0.686	1185	0.862	0.0650	0.963	0.0106	0.137	0.426
9		Ab_4Fa_{96}	0.680	1196	0.943	0.025	0.995	0.042	0.056	0.470
10		$Qz_{56}Ne_{26}Wu_{18}$	0.728	1100	0.191	0.418	1.832	0.0399	0.279	0.088
11		$Qz_{60}Ne_{32}Wu_8$	0.798	980	0.081	1.092	1.020	0.046	0.328	0.037
12		$Qz_{22}Ne_{57}Wu_{21}$	0.755	1050	0.227	0.644	0.883	0.091	0.638	0.111
13	Qz-Ne-Wu	$Qz_{25}Ne_{36}Wu_{39}$	0.728	1100	0.462	0.336	0.756	0.061	0.431	0.227
14		$Qz_{24}Ne_{12}Wu_{64}$	0.702	1150	0.872	0.060	0.684	0.023	0.165	0.439
15		$Qz_{42}Ne_8Wu_{50}$	0.702	1150	0.634	0.198	0.942	0.014	0.102	0.304
16		$Qz_{43}Ne_{45}Wu_{12}$	0.785	1000	0.124	0.907	0.871	0.067	0.471	0.058
17		$Qz_{59}Ne_{35}Wu_6$	0.798	980	0.060	1.223	1.377	0.050	0.356	0.027
18		$Qz_{40}Wu_{48}Cd_{12}$	0.695	1165	0.595	0.225	1.159	0	0	0.283
19	Qz-Wu-Cd	$Qz_{26}Wu_{66}Cd_8$	0.683	1190	0.910	0.041	0.970	0	0	0.455
20		$Qz_{34}Wu_{56}$	0.678	1120	0.908	0.042	1.078	0	0	0.448
21		$Qz_{25}Wu_{67}Cd_8$	0.674	1210	0.588	0.032	1.145	0	0	0.466
22	Qz-Fa	$Qz_{38}Fa_{62}$	0.688	1180	0.603	0.220	1.321	0	0	0.245
23		$Qz_{62}Fa_{38}$	0.677	1205	1.000	0	1.000	0	0	0.500

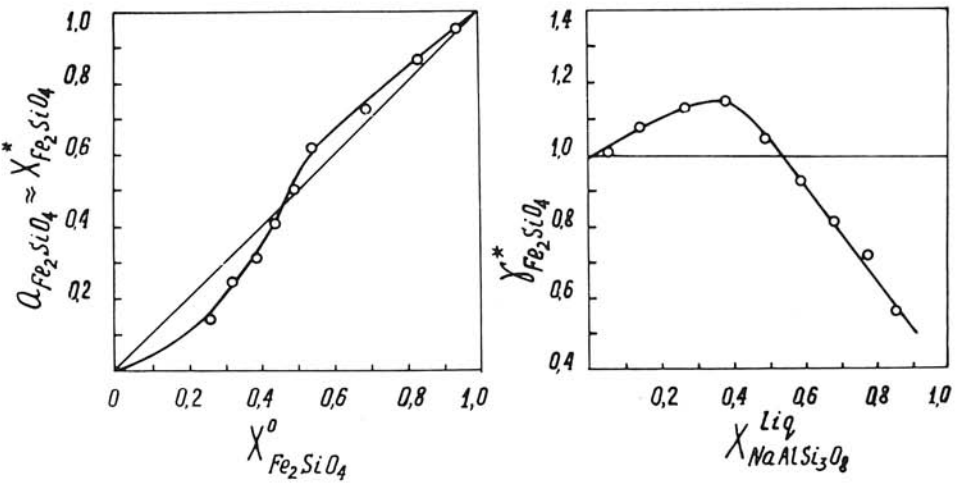

Fig. 3. The dependence of provisional activities and activity coefficient for Fe_2SiO_4 on the melt composition in the system Fa-Al, atm. pressure.

is a mole fraction of the olivine component in the melt. It means that the expression from Tab. 2 can be written as:

$$X^{Liq}_{01} = 3.5\,(Mg + Fe + Mn) : \sum_i A_i \qquad (16)$$

At $X^{Liq}_{01} > 0.4$ this value could be used to evaluate the crystallization temperature of the cotectic mixture. For the alkali-bearing systems with high Mg/Mg + Fe and at $X^{Liq}_{01} < 0.4$ a correction is needed for the activity coefficient. Therefore, we calculated normative Ab in the system and found $\gamma^*_{Mg_2SiO_4}$ from eq. (13). Then we found the $\gamma^*_{(Mg, Fe)_2SiO_4}$ value, and the olivine mole fraction in the ideal mixture was obtained with the equation

$$X^O_{(Mg, Fe)_2SiO_4} = X^*_{(Mg, Fe)_2SiO_4} \cdot \gamma^*\,(Mg, Fe)_2SiO_4 \qquad (17)$$

Such corrections are meaningful for systems with $X^{01}_{Mg} > 0.7$. At decreasing Mg/Mg + Fe of the mixture, the 01 activity coefficient either approaches unity or is positive/negative. This eliminates the need in corrections.

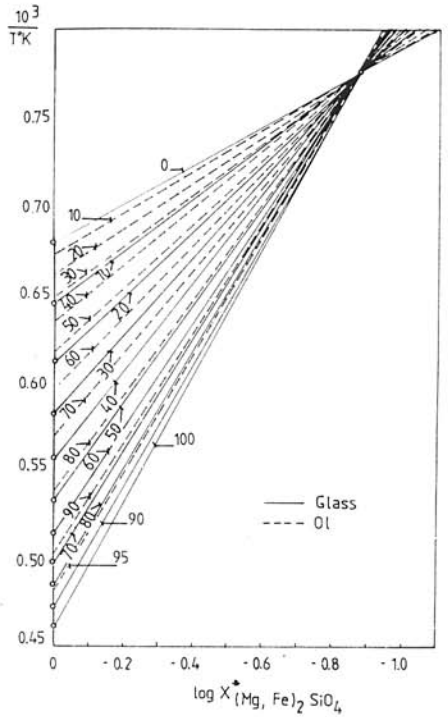

Fig. 4. The relationship between olivine mole fraction in cotectic melt and the Mg/(Mg+Fe) ratio of 01 and reciprocal temperature, 1 atm. pressure.

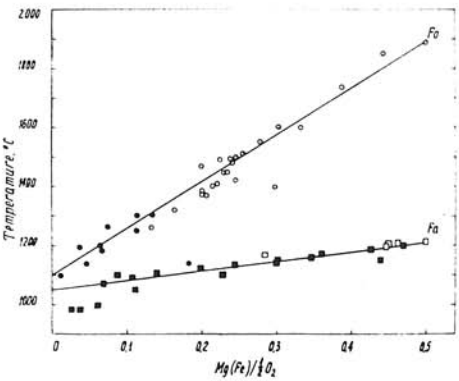

Fig. 5. The Mg:1/2 O_2 and Fe:1/2 O_2 — temperature dependence in cotectic systems with forsterite and fayalite, respectively (from tables 1 and 2).

Knowing Mg/Mg + Fe for 01 and its mole fraction in the system, we can establish the crystallization temperature of magma at atmospheric pressure. Let us, for example, calculate the temperature for the peridotite (sample No. 94273) from New Zealand. Its chemical analysis and olivine composition are described by Challis 1965). Tab. 4 gives the detailes of calculation.

Table 4

Calculation of olivine-bearing basalt composition at $X^{01}_{Mg} = 0.825$

(Columbia River, USA, Roeder, 1974)

Oxides	Wt. %	Molecular quantity	Number of atoms	Number of oxygen atoms	Compositions and temperature
SiO_2	47.34	0.789	2.367	1.578	$X^{rock}_{Mg} = 0.610$
TiO_2	0.83	0.013	0.039	0.026	
Al_2O_3	17.96	0.176	0.880	0.528	$X^*_{01} = 0.291$
FeO	10.30	0.145	0.290	0.145	
MgO	9.44	0.234	0.468	0.234	$\log X^*_{01} = -0.536$
MnO	0.26	0.004	0.008	0.004	
CaO	11.24	0.200	0.400	0.200	$t = 1249\ ^\circ C$
Na_2O	1.56	0.025	0.075	0.025	
K_2O	0.19	0.006	0.018	0.006	
Σ	99.12	—	4.545	2.696	

Table 5

Data on basalt crystallization temperatures (compositions of rocks, olivine and t_0 from Roeder's data, 1974)

No. sample	X_{Ab}	X_{ol}	$-\log X^*_{ol}$	$100\ X^{rock}_{Mg}$	$100\ X^{ol}_{Mg}$	$\frac{Mg+Mn+Fe}{1/2\ O_2}$	Temperature, °C: exp (t_0)	t_1 from Fig. 4	$t_1 - t_0 = (\Delta t_1)$	$t_1 + \Delta t_1$	t_2 from Fig. 6	$t_2 - t_0$
G1—C—71—45	0.049	0.437	0.357	26.2	57.9	0.212	1213	1213	0	1224	1230	+17
G1—C—71—44	0.018	0.437	0.360	38.9	70.0	0.208	1260	1256	—4	1268	1260	0
P—340409—43	0.105	0.208	0.681	48.1	76.0	0.100	1158	1106	—52	1182	1180	+22
WRAB—39	0.046	0.311	0.507	55.0	(79.5)	0.240	1246	1206	—40	1247	1350	+4
WRAB—38	0.050	0.291	0.536	61.0	82.4	0.142	1249	1205	—44	1252	1255	+6
CA4—37	0.067	0.254	0.585	55.4	78.8	0.122	1211	1164	—55	1227	1215	+4
K30J—36	0.047	0.243	0.615	60.8	82.9	0.118	1258	1156	—98	1266	1210	—38
G1—1868—35	0.015	0.381	0.419	63.1	82.5	0.180	1303	1168	—269	—	1300	—3
4136—34	0.174	0.141	0.850	57.1	(81)	0.070	1153	1034	—119	1144	1160	+7
G1—1050—32	0.032	0.844	0.074	26.4	(53)	0.214	1210	1009	—201	—	1215	+5
G1—1050—31	0.027	0.400	0.398	32.8	60.2	0.188	1211	1902	1221	1210	1110	—1
HAW—30	0.161	0.164	0.763	51.2	77.8	0.077	1154	1052	—102	1154	1155	+1
G1—654—28	0.046	0.395	0.403	30.8	60.4	0.190	1210	1012	—198	—	1225	+15
G1—654—27	0.030	0.265	0.577	59.9	(82)	0.151	1251	1176	—75	1231	1253	+2
G1—654—26	0.023	0.456	0.341	34.3	62.2	0.218	1261	1265	+4	1273	1255	—6
4135—25	0.048	0.329	0.483	60.7	82.2	0.141	1250	1175	—75	1212	1250	0
4135—23	0.027	0.381	0.419	35.5	66.3	0.181	1257	1213	—44	1257	1230	—27
KI4G—22	0.074	0.202	0.696	55.2	77.8	0.100	1210	1104	—106	1183	1185	—25
KI4G—21	0.046	0.166	0.779	58.8	82.1	0.126	1254	1064	—190	—	1255	+1
KI4G—20	0.041	0.311	0.508	63.4	83.5	0.147	1306	1226	—80	1268	1260	—46
CRB4A—18	0.064	0.250	0.601	36.4	63.5	0.126	1160	1120	—40	1180	1180	—20
CRB4A—17	0.055	0.251	0.600	40.0	66.4	0.119	1160	1140	—20	1200	1180	+26
CRB4A—15	0.067	0.295	0.531	30.8	57.2	0.141	1162	1143	—19	1189	1180	+18
CRB4A—14	0.067	0.170	0.768	65.8	85.2	0.080	1164	1073	—91	1167	1190	+24
CRB4A—13	0.038	0.245	0.610	44.8	71.9	0.115	1163	1140	—23	1203	1180	+17
SY—MN—8	0.015	0.393	0.406	27.4	54.7	0.186	1154	1189	—35	1210	1205	+51

Tab. 5 shows t_1—t_0 calculated in comparison with the experimental data by Roeder (1974). In the same cases there are great differences between these two estimates of temperature for one of the same sample.

The melting temperatures of oxygen compounds and mixtures are known to increase with the rise in metal/oxygen ratio, i. e. with diminishing Me — O bounds. (Perchuk — Vaganov, 1978). These relationships are very distinct in simple silicate systems. In Fig. 5 the abscissa is the ratio Me: 1/2 O_2 for systems with Fa and Fo on cotectic. This pattern in the metal/oxygen ratio makes it possible to calculate the diagram for the system with varying Fe:Mg ratio. For this we used Bowen and Shairer's (1935) diagram and determined the log $X^{Liq}_{Mg_2SiO_4}$ and $X^{Sol}_{Mg_2SiO_4}$ values which were plotted at 10 mol. % intervals in the diagram in Fig. 6. Mg:1/2O_2, depending on the temperature. The isolines for 01 and glass compositions are plotted from the values of linear dependence of y = (Fe + Mg + Mn): 0.5 O_2 on the temperature (Fig. 5).

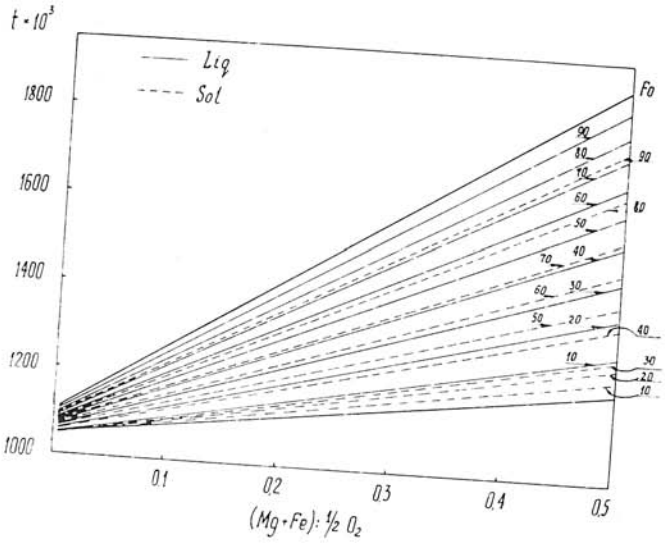

Fig. 6. The lines for identical Mg (Mg+Fe) ratios in equilibrium olivine and melts in the diagram (Mg+Fe+Mn) : 0.5 O_2 vs. temperature.

The t_2—t_0 values are very small and have opposite signs (Tab. 5). The mean error in the temperature determination (Fig. 6) is $\Delta t = 2.077$ °C as compared with Roeder's experimental data (1974), and t_2—t_0 does not depend on the composition of the system. Therefore, the liquidus temperatures of basalts can be estimated straight from the diagram of Fig. 6. It is only necessary to know the compositions of a rock, olivine or glass. The following polinomial can be used in analytical determinations of t°

$$t(°C) = 1039.62 + 43.7368\, X^{01}_{Mg} + 353.86_y + 0.001182\,.\,(100\, X^{01}_{Mg})^2 +$$

$$+ 0.125186_y\,(100\, X^{01}_{Mg})^2 - 0.000031_y\,(100\, X^{01}_{Mg})^3, \quad (18)$$

where

$$y = (Mg + Fe + Mn)/0.5\, O_2 \quad (19)$$

Using Roeder's data we have established the relation between Mg/Mg + Fe of olivine and host basalt,

$$X^{01}_{Mg} = 3.15\, X^{rock}_{Mg} / (1 + 2.15\, X^{rock}_{Mg}). \quad (20)$$

However, Green — Ringwood (1967) found equal Mg/Mg + Fe ratios for both basalts and olivines from them. Olivines and many ultramafic rocks (peridotites and, of course, dunites) have practically the same Mg/Mg + Fe.

Eq. (18) is only valid for anhydrous liquidus estimates, because they have been derived from the data on cotectic ratios in dry melting systems. The introduction of water reduces the liquidus temperature in the same proportion, i. e. with the water content of the rock. The method for calculating liquidus temperatures allows for the H_2O in the t °C estimates. We can compare the calculated and experimental data on the melting of peridotite at 5.73 wt. % H_2O (Millhollen — Irving — Wyllie, 1974):

SiO_2 — 42.22; TiO_2 — 0.30; Al_2O_3 — 4.42; Fe_2O_3 — 2.86; FeO — 4.45, MgO — — 34.61; MnO — 0.13; CaO — 3.92; Na_2O — 0.43; K_2O — 0.11; H_2O — 5.73; Total —99.18.

The liquidus temperature for the dry peridotite calculated from eq. (18), i. e. recalculated anhydrous to 100 %, is 1640 °C, whereas the experimental value is t ≈ 1650 °C. At 5.73 wt. % water the calculated temperature is 1555 °C ± 25. According to Millhollen — Irving — Wyllie's data (1974), individual olivine crystals were noted in the melt at 1550 °C, P = 30 kb. It means that 5.73 wt. % H_2O introduced into the system, reduced the calculated liquidus temperature by ~ 100 °C. The pressure of 30 kb was needed to introduce water into metal at 1550 °C.

The estimated and experimental temperatures for the sample of a hornblende mylonite (Millhollen — Wyllie, 1974) agree well: SiO_2 — 36.64; TiO_2 — 3.99; Al_2O_3 — 19.84; Fe_2O_3 — 2.78; FeO — 8.88; MgO — 6.48; MnO — 0.13; CaO — 13.30; Na_2O — 3.85; K_2O — 0.80; H_2O — 3.55; Total 100.24 wt. %.

The experiments were done in sealed capsules without the preliminary dehydration of the sample. The liquidus temperature was ~ 1180 °C. The liquidus temperature of this sample with 3.55 wt. % water calculated by eq. (18) was 1203 °C, which approaches closely the above value.

The well-known sample of No. M5 olivine-tholeiite from the San Juan, New Mexico (Kennedy, 1948; Yoder — Tilley, 1962; Cohen — Ito —

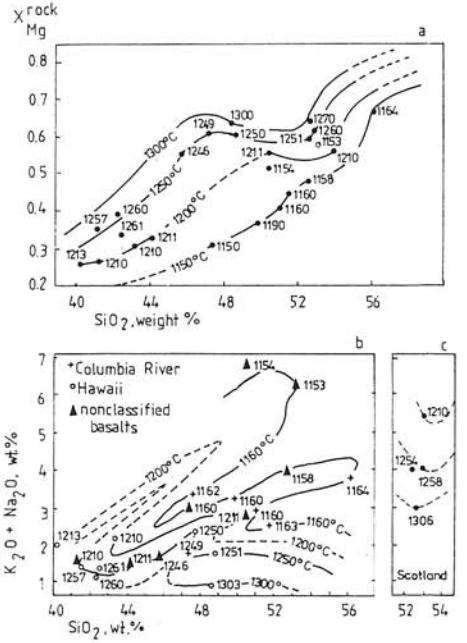

Fig. 7. Correlation between the liquidus temperatures of basalts and their composition (after Roeder, 1974) X^{rock}_{Mg} = = Mg:(MgO+FeO) is the MgO mole fraction in the melt.

Kennedy, 1967) changes completely to melt at t ~ 1200 °C and 1 atm. pressure. Fig. 4 and eq. (18) gave 119 and 1192 °C, respectively. The temperature of 1216 °C was estimated for the intermediate oceanic olivine-tholeiite closely approximating this basalt (Engel et al., 1965).

Temperature regime of differentiation of mafic magmas

Very important geochemical laws have been established on the formation of magma series in a number of now standard works (Walker — Poldervaart, 1949; Mohr, 1960; Wager — Brown, 1970; Yagi, 1953; Kuno, 1960; Kutolin, 1972 and others). Korzhinskii (1959) formulated the principle of acid-base interaction of components in silicate melts, which made it possible to explain many of these laws. Thus, the acid-base interaction enables us to explain the differentiation trends in the diagram FeO-MgO—(Na_2O + + K_2O) for the basalt series as well as the trends in crystallization in the system diopside-hedenbergite-aegirine (Perchuk, 1962, 1964). Consider the relationship between geochemical and temperature regimes of differentiation of basalt magmas. Evidently, such a relationship is to be found in the temperature range equal to the difference of liquidus temperatures in ultrabasite and fayalite-granophyre, i. e. the differentiation is possible in the range of 1600—1050 °C. The most intensive separation of olivine and rhombic pyroxene and a simultaneous formation of ultra-basic rocks and peridotite nodules must occur in the range of 1600—1300 °C. The differentiation of the basalt series proper by crystallization and the formation of acid or alkaline residue occurs in the temperature range of 1300—1050 °C.

The diagrams in Fig. 7 summarize R o e d e r ' s data on liquidus temperature for basalts of varying initial composition. The upper diagram demonstrates the positive correlation between the Mg/Mg + Fe ratio of rocks and their SiO_2 content. This unusual relation is only due to entirely casual selection of samples and does not reflect any pattern in differentiation. However, liquidus temperatures decrease regularly with increasing SiO_2 and FeO in rocks. The lower

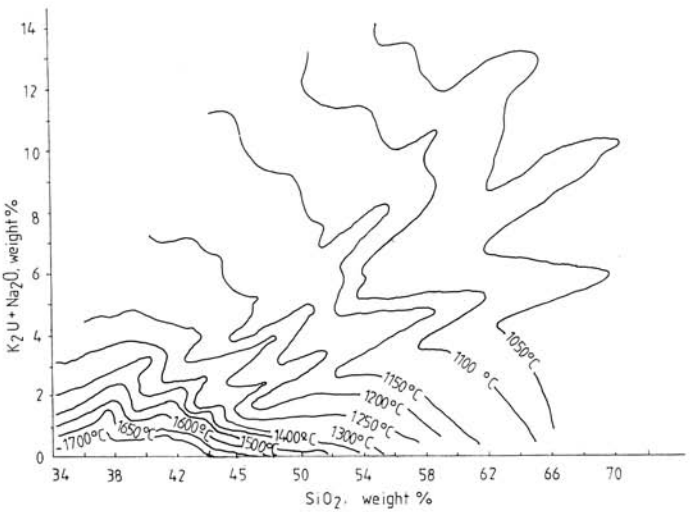

Fig. 8. Approximate isotherms for the liquidii of basalts in the diagram alkali-silica, calculated with help of eq. (21) using the rock compositions published (S c h e i n m a n n, 1968; W a g e r — B r o w n, 1970; C o a t s, 1968 et al.).

diagrams reflect an attempt to use a trend-analysis to find similar relations for alkalis and SiO_2. This attempt is seen to have lead to a quite unexpected result-separate temperature troughs, or projections, of cotectic minima. It means that the liquidus temperature decreases abruptly at some value of the derivative $\frac{\delta m\,(K, Na)_2O}{\delta m\,SiO_2}$, which to some extent relates to other parameters of basalt composition. Even for rocks with ~ 41 % SiO_2 and about 1 % alkali, the liquidus temperature is only 1260—1250 °C. This is because of the high Fe/Mg ratio in certain basalts and the relatively high Al_2O_3 content. If we admit that such 'temperature troughs' reflect the cotectic character of basalt magma crystallization, the physico-chemical nature of the magmatic series outlined by K u n o (1960) becomes clear. This could be verified by estimating liquidus temperatures (with 01) from a very large number of petrochemical data by eq. (18). In other words, a strictly definite position of a cotectic minimum (trough) should correspond to each initial magma composition (relative to Al, Ti, Fe, Mg, Ca and Mn). However, if tholeiite, high-alumina and alkali basalt series exist, there must be corresponding cotectic lines in the diagram $(Na_2O + K_2O) — SiO_2$. The trend-analysis for 159 samples produced temperature troughs with the mean correla-

tions coefficient of 0.41 (Fig. 8). This is a high enough value to indicate that isotherms in Fig. 8 are only approximate. This implies that the position of cotectic minima in the diagram is not fixed and that the shape of the isotherms might vary considerably. This is not surprising, because, in general, a shifted cotectic will not produce the projection of a minimum. But in this particular case (Fig. 8) certain patterns have come to light in the natural magma evolution in different geostructural zones, that is, some general conditions of magma differentiation in plateaus, volcanic islands, and in the early stages of the rift structure development. As a result, a cotectic character of crystallization differentiation of basic magmas is very distinct, and enables us to analyse the regional rock series with olivine on the liquidus. Here K u n o (1968) distinguished three series: tholeiite, high-alumina and alkali. The diagram in Fig. 8 only covered part of the calc-alkali rock series (gabbro-diorite-granophyre; basalt-andesite-dacite-rhyolite). Only the rocks with olivine on the liquidus could be shown.

To reveal the causes of the cotectic minima shift in the diagram alkali-silica, we must compare various differentiation series of basalt magma. This can conveniently be done with the regional series of common magmatic rocks.

The Karroo province: W a l k e r — P o l d e r v a a r t (1949) studied this province in detail. The Karroo dolerites occur in dikes, layered intrusions and sheets produced by crystallization of the tholeiite magma. Though picrite and acid rocks are present in small quantities, the authors clearly proved a distinct differentiation on the basis of field observations and innumerable rock chemical analyses. According to these authors, certain acid varieties were produced by the reomorphism of the enclosing sedimentary rock, under the effect of the tholeiite magma emanation.

The diagrams in Fig. 9 show a complete differentiation of the Karroo dolerites. The triangular diagram is taken from the work of W a l k e r — P o l d e r v a a r t (1949). Later K u n o (1968) took the Karroo dolerites as a basis for distinguishing the tholeiite series of basalt magmas, for which he used the $(Na_2O + K_2O) — SiO_2$ diagram. The compositional points for all magmatic rocks of the region in question are given in the same coordinates in Fig. 9. The temperature isolines reproduced from Fig. 8 emphasize the peculiarities of the differentiation of this tholeiite magma. The compositional points are situated along two temperature troughs. This means that differentiation proceeded along two cotectic lines, the common tholeiite and high-alumima basalt (K u n o, 1960). Picrites and acid rocks are also present in the both series, so the differentiation is more or less complete. But one of these series was formed at somewhat higher alkali potentials (K and Na) and slower temperature rates of differentiation, i. e. it is more strongly differentiated. However, in the absence of evidence for a direct relation between acid rocks and dolerite magma (according to W a l k e r — P o l d e r v a a r t, 1949 these rocks are of uncertain nature), this conclusion is only tentative.

The differentiation of high-alumina magma has been considered by K u n o (1960, 1968) on the analytical material for basalts from central Japan, Skaergaard, Beaver-Bay etc. K u n o also studied the differentiation of the tholeiite magma on the basalts from Palisades, Dillsburg and Okata. These regional series obey fairly well cotectic crystallization, i. e. they meet the respective projections of cotectic minima in Fig. 8.

The Sidara mugearites in Japan closely approach high-alumina basalts (K u n o, 1960, 1968). The differentiation stages from olivine basalts to dolerite pegmatites and microsyenites are seen clearly on the boundary between the alkali and high-alumina basalts in the alkali-silica diagram in Fig. 9. We shall not consider these stages here, because they were discussed in much detail by K u n o (1960, 1968).

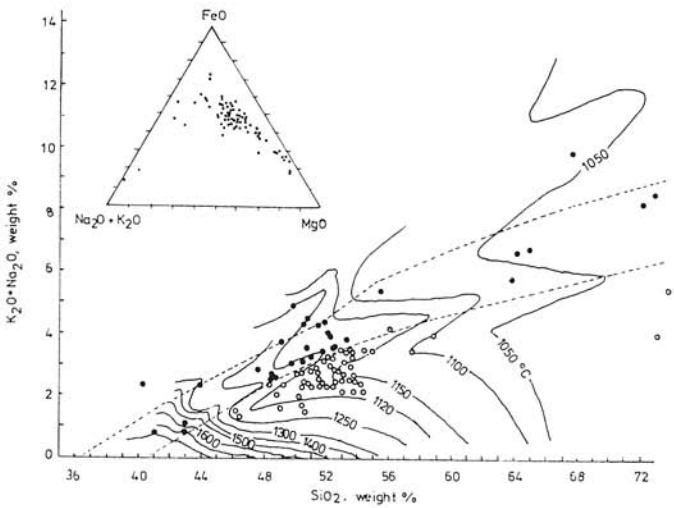

Fig. 9. Differentiated volcanic series of high-alumina (1) and tholeiite basalts (2) from the Karroo dolerites, South Africa.
Explanations: The triangular diagram shows the differentiation stages in rocks within the coordinates (K_2O+Na_2O)—FeO—MgO (after W a l k e r — P o l d e r v a a r t, 1949). The dotted lines show boundaries between tholeiite and high-alumina basalts and between high-alumina and alkaline basalts (K u n o, 1960).

The series of alkali olivine basalts and the products of their differentiation show a great variety of compositions and types of cotectic crystallization. We will consider several distinct types of differentiation in greater detail.

Alkali rocks of Morotu, Sakhalin: Y a g i (1953) gives a detailed description of this intrusive complex. Dolerites, monzonites and syenites are common constituents for many rock types. Dolerites contain often iron-rich olivine; monzonites and syenites are olivine-free rocks, but olivine could be expected to appear on the liquidus in these rocks. We then can show the differentiation series of the Morotu district in the alkali-silica diagram, by projecting the liquidus of alkali olivine rocks. The diagram (Fig. 10) shows the way of crystallization differentiation of alkali-basalt magma for this region. This way defines clearly the projection of the cotectic minimum on the plane between the chosen coordinates, and shows higher liquidus temperatures than those in Fig. 8.

The Morotu river alkali province is not the only example of differentiation of alkali olivine basalt (K u n o, 1968). The shift of the temperature trough into the alkaline region is best seen when analysing African traps.

The Ethiopian trap formation: Described in detail by M o h r (1960). Two of the most distinct differentiation series of basalt magmas of increased alkalinity could be distinguished here.

1. Picritic basalt (tholeiite) — alkali olivine basalt-trachyandesite-Na trachyte-alkali trachyte-anortite trachyte SiO_2 $(Na_2O + K_2O) \approx 5.5$.

2. Olivine basalt-trachyte-pantelerite-bostonite-rhyolite-quartz-bostonite-paisanite (alaskite) $SiO_2 : (K_2O + Na_2O) \approx 8$.

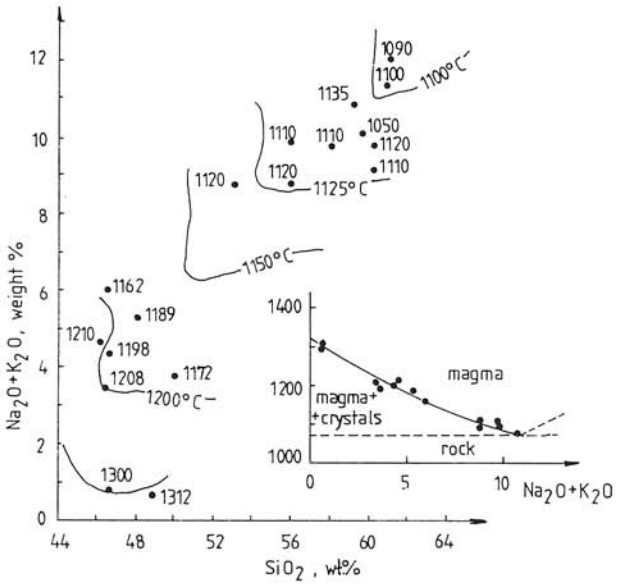

Fig. 10. Cotectic differentiation of alkali basalt magma is Morotu River district, Sakhalin.

We can see that in the first series the differentiation of basalts produced nepheline rocks, i. e. with pronounced silica undersaturation. We could call this differentiation series phonolitic. The differentiation of the second alaskitic series, resulted in silica-oversaturated rocks, relatively rich in alkalis.

Consider the first of these series. The compositional points are plotted in the alkali-silica diagram (Fig. 11). The visible basalt magma crystallization trend approaches the projection of the cotectic minimum in the basalt anhydrous system closely (Fig. 8). We can derive the liquidus for this system from the SiO_2-alkali relationship in the temperature-alkali diagram. This simplified diagram is given in the insert in Fig. 11. The uetectic seems to show up at 1150 °C and $Na_2O + K_2O = 13.5$ wt. %.

This differentiation series of alkali basalt magma in the Ethiopian trap formations is only slightly different from the Atumi, Morotu and Gough island and other formations by $SiO_2/(Na_2O + K_2O)$ ratio. Nevertheless, it produces more strongly differentiated rocks, up to phonolites and phonolite trachytes.

The series from picrites and basanites to leucite basalts and leucite phonolite trachybasites appear to be the most alkaline. Unfortunately, there are no classified data on petrochemistry of these differentiation series. Therefore, we shall confine ourselves to Zavaritskii's (1960) and Scheinmann's data (1968) on the composition of the most alkaline plateau basalts. Tab. 6 shows that these rocks have high alkali-to-silica ratios — 0.169 to 0.251. These values could be com-

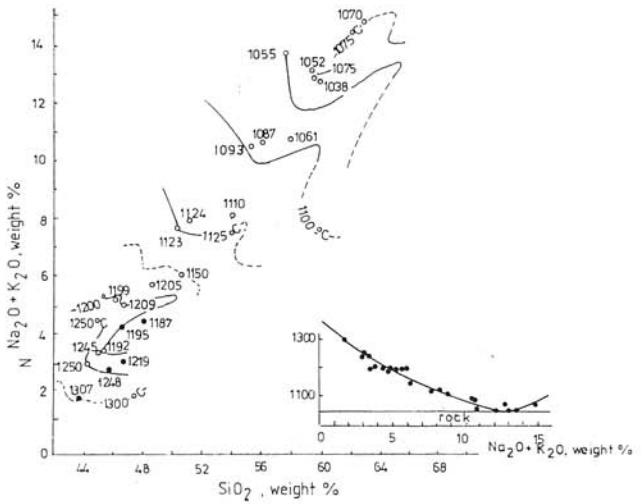

Fig. 11. Cotectic differentiation of highly alkaline magma in the Ethiopian trap formation.

Table 6

Compositions and liuqidus temperatures of rocks in the possible series of the most alkaline differentiation

Rock	100 X^{01}_{Mg}	Mg + Fe + + Mn 1/2 O_2	t °C eq. (18)	SiO_2 wt. %	$Na_2O + K_2O$ wt. %	$\frac{Na_2O + K_2O}{SiO_2}$
Missourite	90.6	0.167	1317	44.27	5.5	0.124
Leucite basalt	86.0	0.120	1239	46.18	8.54	0.198
Fergusite	85.5	0.077	1182	48.97	9.68	0.198
Leucite	82	0.079	1178	46.90	10.37	0.221
Kenyte	44	0.016	1060	53.77	12.27	0.228
Phonolitic trachibasalt	12	0.040	1065	55.62	13.97	0.251

pared with the data for the above differentiation series, which is best done by a diagram. Fig. 12 compares five series, or types, of differentiation, which are the projections of cotectic minima on the alkali-silica plane in a complex basalt system. These projections when extrapolated into the low region of SiO_2 and K_2O values will intersect at SiO_2 = 42.7 wt. % and $Na_2O + K_2O$ = 1.2 wt. %.

This intersection suggests the various trends of differentiation of basalts, while indicating that they are produced by a partial melting of the mantle rocks with the previously mentioned alkali and silica contents. In the literature we could find a composition closely approximating that of a lherzolite bomb from Madeira (S c h e i n m a n n, 1968).

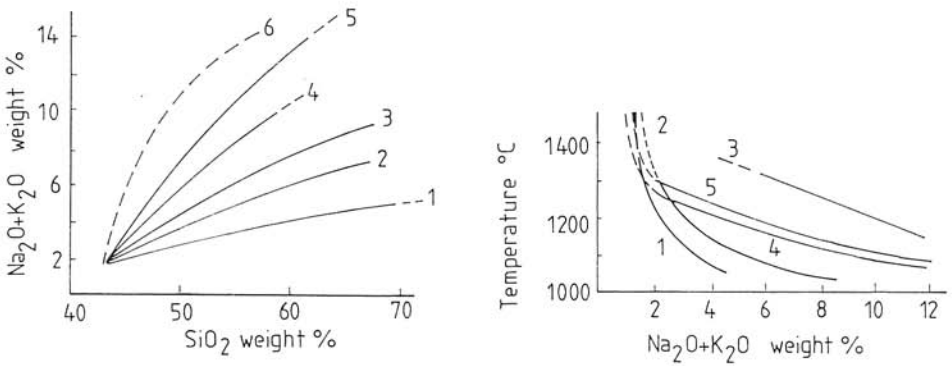

Fig. 12. The comparison of differentiation stages of various basalt magmas. Dashed lines — boundaries of basalt series (after K u n o, 1968). Crosses are for average compositions of predominant ultramafic rocks and nodules in basalts.
Explanations: Karroo type: 1 — tholeiitic series; 2 — highly alumina series; 3 — Sidara type; 4 — Morotu type; 5 — Ethiopia type; 6 — possible highly alkaline type.

Consider possible causes of the displacement of cotectic minimum in the silica--alkali diagram. K u n o (1968) suggested that the magmatic rock series are produced by fusion and differentiation of basalt magma at various depths.

K u n o has demonstrated on the petrochemical analyses of basalts of Japan that the alkali olivine basalts from the western part of the Japanese island arc melt at greater depths as compared with the generation of high alumina and tholeiite basalt magmas. The locations of the deep-focus earthquake epicentra in the Beniof zone correlate with the melting zones of the respective magmas.

The present study supports this elegant K u n o's model to a certain extent. The shift of the cotectic minimum might have been due to the pressure increase, i. e. the higher the pressure, the more alkaline magmas are fused from the mantle of the Earth. The true tholeiite series (differentiation series of Karroo, Sidara etc.) are formed in rift zones of the continents, ridges etc. These magmas are generated at shallow depths. Each of the subsequent types of differentiation occurs on a more consolidated crust, until, finally, series associated with traps and plateau volcanoes, develop. For these series maximum depths of magma generation are expected (P e r c h u k, 1973; M a r a k u s h e v — P e r c h u k, 1975).

Experimental data on the melting and differentiation of basalt of varying compositions (Y o d e r — T i l l e y, 1962; G r e e n — R i n g w o o d, 1967; C o h e n — I t o — K e n n e d y, 1967) suggest the possible great depths of the alkali basalt melting. This is seen from the direct comparison of dry liquidi of

the three main types of basalt at a constant temperature. However, pressure is unlikely to be the only factor responsible for the abrubt shift of the cotectic minima into the region of differentiation of alkali-rich series with the formation of phonolites, leucite-phonolites, etc.

In developing the chemical model of the Earth's interior (Marakushev — Perchuk, 1971, 1975; Perchuk, 1976) we came to a conclusion that the generation of alkali magmas and the displacement of the cotectic minimum in the diagram alkali-silica are due both to pressure and high alkalinity of juvenile fluid. The increase in the pressure has been shown (Perchuk, 1976) to lead to the decomposition of solid compounds of alkali metals with gases (MeH, MeF, MeCl, Me_2O, Me_2S etc.). As a result, alkaline gaseous fluids are formed, and the temperature of basalt melting from the mantle substrate decreases. These fluids carry magma to the surface of the Earth in much the same manner as the gas drill performs. On their way to the surface of the Earth the gas streams are oxidized, producing H_2O, CO_2 and releasing excess energy which is consumed by partial melting of rocks from the mantle and crust.

This hypothesis seems to agree well with our data on the shift of the cotectic minimum (trough) in the diagram alkali-silica.

The suggested model of calculation of liquidus temperatures of mafic and ultramafic rocks is for the systems which do not contain gaseous phase, 1 atm. pressure. However, analyses of numerous data on rock compositions and temperatures of the beginning of crystallization of these rocks have led us to conclusions that are beyond the limits imposed by the conditions. There are not any contradictions here though. Taking the melting temperature of a rock at 1 atm. as a standard, we have determined the patterns of the cotectic deviation from this standard. This explains the intricate shape of the isotherms in Fig. 8.

Concluding remarks

The methods of mineralogical thermometry, presented in this paper, make it possible to quantitatively evaluate the temperature regime of differentiation of mafic magmas within each continental series distinguished by Kuno (1968). Therefore, we were able to show the correlation between SiO_2 and the sum of alkalis for each given differentiation series as the projection of the cotectic minimum on the plane within the given coordinates and also demonstrate the effect of pressure and alkalinity of juvenile fluids on this minimum.

The comparison of differentiation series within the regional series of magmatic rocks suggests the common source of basic and alkaline magmas in the mantle of the Earth; the composition of the mantle should correspond to lherzolite with 43 wt. % SiO_2 and 1.2 wt. % alkali. Consequently, hyperbasite and kimberlite intrusions with $Na_2O + K_2O$ less than 1 wt. % are in relation to the primary mantle (Fig. 12). Klushin — Abramovich (1975) came to a similar conclusion. They studied the evolution of the composition of alpino-type hyperbasites within the certain regions. These authors have found the Al, Ca and alkali contents in these intrusions to decrease and the Mg/(Mg + Fe) ratio to increase as the absolute age of these intrusions diminishes. So the conclusion has been drawn that the alpino-type hyperbasites are of the restite character and that their composition changes from lherzolite or harzburgite to dunite one.

Consequently, various methods used to investigate basic rocks, indicated the intimately associated evolution of these rocks as well as the primariness of the ultramafic magmas, i. e. the products of complete mantle melting. The methods of mineralogical thermometry make it possible to estimate the magma temperature regime from liquidus till subsolidus, when a porous fluid disappears from the rocks.

REFERENCES

BOWEN, N. L. — SCHAIRER, I. F., 1935: The system MgO-SiO_2-FeO. Amer. J. Sci., 2, pp. 151—217.

BOYD, F. R., 1969: Electron-probe study of diopside inclusions from kimberlite. Amer. J. Sci., 267, A, pp. 50—69.

CHALLIS, G. A., 1965: The origin of New Zealand ultramafic intrusions. J. Petrology, 2, pp. 322—362.

COHEN, L. — ITO, K. — KENNEDY, G., 1967: Melting and phase relations in an anhydrous basalt to 40 kilobars. Amer. J. Sci., 6, pp. 519—539.

DAVIS, B. T. — BOYD, F. R., 1966: The join $Mg_2Si_2O_6$-$CaMgSi_2O_6$ at 30 kb pressure and its application to pyroxenes from kimberlites. J. Geophys. Res., 71, 14, pp. 3567—3576.

ENGEL, A. E. — ENGEL, C. G. — HAVES, R. G., 1965: Chemical characteristic of oceanic basalts and the upper mantle. Bull. Geol. Soc. Amer. 76, pp. 719—734.

GREEN, D. H. — RINGWOOD, A. E., 1967: The genesis of basaltic magmas. Contrib. Miner. Petrology, (Berlin—New York), 15, pp. 103—190.

GREEN, D. H. — RINGWOOD, A. E., 1970: Mineralogy of peridotitic compositions under upper mantle conditions. Phys. Earth Planet. Interiors., 3, pp. 359—371.

HESS, H. H. — POLDERVAART, A. ed., 1968: Basalts. Interscience publishers. New York-London-Sydney.

KENNEDY, G. C., 1948: Equilibrium between volatiles and oxides in igneous rocks. Amer. J. Sci., 246, pp. 529—549.

KLUSHIN, I. G. — ABRAMOVICH, I. I., 1975: To the evolution of the composition of alpine-type hyperbasites. Akad. Nauk USSR, Doklady, 221, 2, pp. 451—453.

KORZHINSKII, D. S., 1959: Acid-base interaction of components in silicate melts and the direction of cotectic lines. Akad. Nauk USSR, Doklady, 128, 2.

KRETZ, R., 1963: Distribution of magnesium and iron between orthopyroxene and calcic pyroxene in natural mineral assemblages. J. Geol., (Chicago), 71, 4, pp. 773—785.

KUNO, H., 1960: High-alumina basalt. J. Petrology, 1, 1, pp. 121—145.

KUNO, H., 1968: Differentiation of basalt magmas. In: Basalts, ed. by Hess, H. H. and Poldervaart. A., Intersci. Publishers, pp. 623—689.

KUSHIRO, I., 1973: Regularities in the shift of liquidus boundaries in silicate systems and their significance in magma genesis. Annual Report of the Director. Geophys. Lab. Carnegie Inst. Y. B. 72, pp. 497—507.

KUSHIRO, I., 1975: On the nature of silicate melt and its significance in magma genesis: regularities in the shift of the liquidus boundaries involving olivine, pyroxene and silica minerals. Amer. J. Sci., 275, 4, pp. 411—431.

KUTOLIN, V. A., 1972: Problems of petrochemistry and petrology of basalts. Nauka, Novosibirsk, 207 pp.

McGREGOR, I. D., 1974: The system MgO-Al_2O-SiO_2: Solubility of Al_2O_3 in enstatite for spinel and garnet peridotite compositions. Amer. Mineralogist, 59, 1—2,, pp. 110—120.

MARAKUSHEV, A. A. — PERCHUK, L. L., 1971: Origin and evolution of metamorphic and transmagmatic fluids. Internat. geochim. Congress, Abstracts, Nauka, Moscow, 11.

MARAKUSHEV, A. A. — PERCHUK, L. L., 1975: The main tendencies in magmatism evolution in the development of crust. In: Crust and upper mantle, Moscow Univ. Press.

MILLHOLEN, G. L. — IRVING, A. J. — WYLLIE, P. J., 1974: Melting interval of peridotite with 5.7 % water to 30 kilobars. J. Geol. (Chicago), 82, 5, pp. 575—587.
MOHR, P. A., 1960: The geology of Ethiopia. Univers. college. Addis Ababa, 268 pp.
MUNOZ, M. — SAGREDO, J., 1974: Clinopyroxenes as geobarometric indicators in mafic and ultramafic rocks from Canary Islands. Contr. Mineral. Petrology (Berlin-New York), 44, 2, pp. 139—147.
PERCHUK, L. L., 1962: The effect acid-base interaction of components in the system aegirite-hedenbergite-diopside. Akad. Nauk USSR, Doklady, 147, 6.
PERCHUK, L. L., 1964: Physico-chemical petrology of granitoid and alkaline intrusions in the Central Turkestano-Alay. Nauka, Moscow.
PERCHUK, L. L., 1968: Pyroxene-garnet equilibrium and the depth facies of eclogites. Int. Geol. Rev., (Washington), 10, 3.
PERCHUK, L. L., 1970: Equilibria of rock-forming minerals. Nauka, Moscow.
PERCHUK, L. L., 1973: Thermodynamics regime of deep petrogenesis. Nauka, Moscow.
PERCHUK, L. L., 1976: Gas-mineral equilibria and a possible geochemical model of the Earth's interior. Phys. Earth Planet. Interiors., 13, pp. 232—239.
PERCHUK, L. L. — VAGANOV, V. I., 1978: Temperature regime of crystallization and differentiation of basic and ultrabasic magmas. In: Contributions to Physico-chemical Petrology, V. VII, Nauka, Moscow, pp. 142—174.
RAMBERG, N. — De VORE, G., 1951: The distribution of Fe** and Mg** in coexisting olivines and pyroxenes. J. Geol. (Chicago), 59, 3, pp. 193—210.
ROEDER, P. L., 1974: Activity of iron and olivine solubility in basaltic liquidus. Earth planet. Sci. Lett., 23, 3, pp. 397—410.
ROEDER, P. L. — EMSLIE, R. E., 1970: Olivine-liquid equilibrium. Contrib. Mineral. Petrology (Berlin-New York), 29, pp. 257—289.
SHEINMANN, Yu. M., 1968: Contributions to deep (abysal) petrology. Nedra, Moscow.
WAGER, L. — BROWN, G., 1970: Layered igneous rocks. (in Russian), Mir, Moscow.
WALKER, F. — POLDERVAART, A., 1949: Karroo dolerites of the Union of South Africa. Geol. Soc. Amer. Bull., 60, pp. 591—706.
WYLLIE, P. L., editor: Ultramafic and related rocks. John Wiley and Sons Inc. New York-London-Sydney.
YAGI, K., 1953: Petrochemical studies on the alkaline rocks of the Morotu district, Sakhalin. Geol. Amer. Soc. Bull., 64, 7, pp. 769—810.
YODER, H. S. — TILLEY, C. E., 1962: Origin of basalt magmas. J. Petrology, 3, 3.
ZIMIN, S. S., 1973: Parageneses of ophiolites and upper mantle. Nauka, Moscow.

Review by B. CAMBEL

Manuscript received May 30, 1983